



Numerical Studies on Thrust Augmentation in High Area Ratio Rocket Nozzles by Secondary Injection

S. Shyji^{1†}, M. Deepu², N. A. Kumar³ and T. Jayachandran⁴

¹ Department of Mechanical Engineering; SCT College of Engineering, Thiruvananthapuram, Kerala-695018, India

² Department of Aerospace Engineering; Indian Institute of Space Sci. &Tech., Thiruvananthapuram, Kerala-695547, India

³ Department of Mechanical Engineering; College of Engineering, Thiruvananthapuram, Kerala-695016, India

⁴ Propulsion & Space Ordnance Entity, Vikram Sarabhai Space Center, Thiruvananthapuram- 695022, India

†Corresponding Author Email: shyjis@gmail.com

(Received October 21, 2016; accepted May 22, 2017)

ABSTRACT

Single stage to orbit propulsion devices are being developed as part of low cost access to space endeavors. Sea level operation of high area ratio rocket nozzle used in rocket engines leads to an overexpanded flow condition resulting in high side loads. Secondary injection of propellants in high area ratio nozzle is an attractive option to overcome the inefficiency of operation of such nozzles in sea level conditions in addition to the augmentation of thrust. A numerical study on thrust augmentation in high area ratio nozzle by secondary injection of propellants is presented here. The turbulent compressible reacting flow in rocket nozzle with auxiliary injection is simulated using conservation equations for chemical species based on finite rate chemistry model and compressible Navier-Stokes equations with AUSM+-up upwind scheme based unstructured finite volume solver. An optimized eight step, six species reduced H₂-O₂ finite chemistry reaction model is used to model the supersonic combustion. The indigenously developed solver has an efficient rescaling algorithm to alleviate the effect of stiffness in conventional explicit algorithm for simultaneous solution of reacting flow. The code is validated using the wall pressure and hydrogen concentration values reported for the similar high area ratio rocket nozzle. Accurate prediction of nozzle performance is possible with present turbulent reacting flow simulation as it take care of all losses in nozzle flow. Extensive computations have been performed for the performance estimation of high area ratio rocket nozzle for various prospective auxiliary injection options.

Keywords: Rocket nozzles; Thrust augmentation; Turbulent reacting flows; AUSM+-up scheme; Finite volume method.

NOMENCLATURE

C	concentration of a species	γ	molecularity of the reaction
D'	diffusion coefficient	ε	kinetic energy dissipation rate
E	total energy	κ	turbulent kinetic energy
H	total enthalpy	μ	dynamic viscosity
h	specific enthalpy	ρ	density
K	thermal conductivity	τ	shear stress
k	rate of chemical reaction	Φ	equivalence ratio
p	static pressure	$\dot{\omega}$	rate of production of species
p_0	stagnation pressure	Subscripts	
Q	heat flux	b	backward reaction
R_u	universal gas constant	f	forward reaction
V	volume of the control volume	i	chemical species
Y	mass fraction of a chemical species	j	reaction step
W	molecular weight of a chemical species	l	laminar
		t	turbulent

1. INTRODUCTION

The performance of a rocket nozzle depends on its ability to deliver the required thrust and specific impulse. The engine requires a high specific impulse to minimize the mass of the propellants required for the mission. This is possible only with a nozzle of very high area ratio for a given propellant combination. But for nozzles with high area ratios, the exit core flow may get over expanded and will reduce the nozzle core exit pressure much below the atmospheric pressure. Therefore, it will affect the performance of the engine during the takeoff from the sea level when the engine thrust demand is maximum. Flow separation due to overexpansion also results in side load generation and thereby creating negative thrusts near to the exit surface of the nozzle. This in turn reduces the expected thrust output during the takeoff at sea level compared to that expected in vacuum condition.

Recently a concept based on secondary injection in rocket nozzle, patented by Aerojet General Corporation known as Thrust Augmentation Nozzles (TAN), is gaining research interest (Forde *et al.* 2006). This is an attractive option to increase lift off thrust without altering main engine design and chamber pressure. The propellants are injected in an annular section of the diverging portion of the nozzle and burns in the supersonic flow. The gas generated by the combustion of the secondary flow near to the wall bring down the effective area ratio of the core nozzle flow. Hence the Mach number of the core flow reduces and nozzle exit pressure increases. This effect shall compensate the momentum losses due to the over expansion of the core flow. In addition to this, the inertia and energy release associated with the combustion of the secondary injection of the propellants contributes to the exit thrust. Hence, thrust augmentation in high area ratio rocket nozzles can be achieved by the added mass, inertia and energies of the secondary injection. This thrust augmentation is theoretically limitless since both propellants are admitted in all possible proportions for combustion. However, this combined effect will account around 40% optimum increase in the thrust output of the nozzle (Davis *et al.* 2006).

Effect of the injection angle, pressure, and fuel-oxidizer ratio of the propellants used in the secondary injection in performance of a high area ratio nozzle is analyzed in the present study. The propellants selected for the study are gaseous hydrogen and gaseous oxygen. Present solver for the solution of reacting flow field is developed using Finite Volume Method (FVM) incorporating RNG K- ϵ turbulence model and optimized H₂-O₂ finite chemistry model. The code is validated using experimental wall pressure and fuel concentration data for combustion in high area ratio nozzle.

2. REVIEW OF LITERATURE

After burning in rocket and air-breathing propulsion

systems has been conceptualized and analyzed by various researchers during the past few decades. Borowski *et al.* (1994) introduced the concept of a nuclear thermal rocket (NTR) augmented with liquid oxygen (LOX) for space transportation systems for lunar mission. Here oxygen alone is injected in the diverging part of the nozzle and thrust is augmented due to supersonic combustion with nuclear preheated hydrogen. Later Bulman *et al.* (2000) conducted experiments with the injection of gaseous oxygen in the down-stream of the throat of a NTR nozzle to study the thrust enhancement. Numerical simulations also have been performed for a hot fire test of the concept and successfully predicted the performance. Later Forde *et al.* (2003) introduced the new concept of Thrust Augmentation in Nozzles (TAN) by injecting both propellants at an annular section on the downstream side of the throat of a high area ratio rocket nozzle. Their experiment results in the improvement of the Nozzle thrust with the secondary injection of propellants by compensating the overexpansion losses in high area ratio nozzles. They (Forde *et al.*, 2006) have also reported outcomes of numerical simulation of the flow field for the thrust augmentation and predicted the improved performance of the Nozzle. Both axisymmetric and three dimensional numerical investigations are in good agreement and predicted that thrust improvement is a function of the augmentation mass flow. Later they have experimentally established the use of dual fuel in thrust augmentation with LOX/RP-1 propellants in an SSTO vehicle driven by seven up-sized Space Shuttle Main Engine (SSME) class engines. Recently Candon *et al.* (2016) conducted studies on thrust augmentation and its optimization in hypersonic air breathing engines using after burners. Oxygen is injected through ramp injectors into the expanding exhaust gas to react with unburnt hydrogen in the exhaust stream to achieve thrust augmentation.

Expeditions on development of fuel delivery systems for air-breathing propulsion devices has promoted research on secondary injections to supersonic free stream. Spaid and Zukoski (1964) studied the flow field around the injection point of secondary injection of a nitrogen, argon or helium gas normal to a supersonic flow with free stream Mach numbers of 1.38 to 4.54 using a series of wind tunnel experiments. Based on the inviscid model of the flow field a scaling law for side force generation was also developed. Aso *et al.* (1991) conducted experiments with gaseous nitrogen sonic injection to a supersonic cross flow of Mach number 3.75 and 3.81 through a transverse slot on a flat plate. Schlieren visualization and static pressure measurements were used for the visualization of the flow field. Aso *et al.* (1994) extended their studies with numerical investigations and results had good agreement with own experimental results. Rizzetta (1992) numerically investigated the same flow field by the integration of unsteady mass-averaged Navier-Stokes equations and K- ϵ turbulence model and successfully predicted the flow field. Gruber *et al.* (1995) studied the mixing and penetration performances in three transverse/oblique,

circular/elliptical injector configurations and with cross-flow Mach Number 2. Later [Everett *et al.* \(1998\)](#) conducted experiments to measure the wall pressure when a sonic jet is injected transversely into a supersonic free-stream Mach number of 1.6 with different momentum flux ratios. It was observed that wall static pressure upstream of the injection point increases with increase in the momentum flux ratios. [Fuller *et al.* \(2000\)](#) conducted experimental investigations for the effect of injection angles on the atomization of the liquid jets in transverse air flow. [Boles *et al.* \(2010\)](#) conducted computational investigations using LES and RANS simulations of sonic injection into a Mach 2 cross stream of air, helium, and ethylene to predict the upstream boundary layer structure. [Gao *et al.* \(2011\)](#) conducted numerical investigations to study the mixing characteristics of various injection schemes when sonic normal jet is introduced into a supersonic free stream cross flow.

Research work on 1030 area ratio Rao contoured DeLaval Nozzle by [Pavli *et al.* \(1987\)](#) formed the basis of the present numerical study as effect of mixing and combustion can be assumed to complete within the higher area ration nozzle flow field. [kacynski \(1994\)](#) conducted experimental studies on the 1030 area ratio Rao contoured DeLaval nozzle with hydrogen and oxygen as the fuel and oxidizer at both atmospheric conditions (sea level conditions) and high altitude conditions (near vacuum conditions) for various performance parameters like thrust, specific impulse, nozzle wall pressure distribution, hydrogen mass fraction etc. His results clearly show the poor performance of the Nozzle at sea level conditions in thrust and Specific Impulse development due to the over expansion of the gas at Nozzle exit compared to the high altitude conditions. He repeated his studies with numerical simulations to study the reacting flow field and estimated the nozzle performance parameters at high altitude conditions.

3. GOVERNING EQUATIONS

Solution of high speed turbulent reacting flows has been carried out using solution of two dimensional Navier-Stokes equation in axisymmetric form with species transport and an optimized eight-step H₂-O₂ finite chemistry reaction model.

$$\frac{\partial \mathbf{U}}{\partial t} + \frac{\partial (\mathbf{F} - \mathbf{F}_v)}{\partial x} + \frac{\partial (\mathbf{G} - \mathbf{G}_v)}{\partial r} = \mathbf{S} \quad (1)$$

where the vector of conservation variable

$$\mathbf{U} = [\rho, \rho u, \rho v, \rho E, \rho \kappa, \rho \varepsilon, \rho Y_i]^t$$

Flux vectors in axial direction are

$$\mathbf{F} = [\rho u, (\rho u^2 + P), \rho uv, (\rho E + P)u, \rho u \kappa, \rho u \varepsilon, \rho u Y_i]^t$$

$$\mathbf{F}_v = [0, \tau_{xx}, \tau_{xy}, Q_x, \mu \kappa \frac{\partial u}{\partial x}, \mu \varepsilon \frac{\partial \varepsilon}{\partial x}, D \frac{\partial Y_i}{\partial x}]^t$$

Flux vectors in radial direction are

$$\mathbf{G} = [\rho v, \rho uv, (\rho v^2 + P), (\rho E + P)v, \rho v \kappa, \rho v \varepsilon, \rho v Y_i]^t$$

$$\mathbf{G}_v = [0, \tau_{xy}, \tau_{yy}, Q_y, \mu \kappa \frac{\partial u}{\partial y}, \mu \varepsilon \frac{\partial \varepsilon}{\partial y}, D \frac{\partial Y_i}{\partial y}]^t$$

The vector of source terms expressed as

$$\mathbf{S} = [0, 0, 0, 0, H_\kappa, H_\varepsilon, S_{Y_i}]^t$$

Effective transport coefficients such as thermal conductivity, viscosity, and diffusion coefficients are estimated in the present solver as the sum of laminar and turbulent values. Laminar viscosity is evaluated using the Sutherland's law and the turbulent viscosity is given by

$$\mu_t = \rho C_\mu \frac{\kappa^2}{\varepsilon}$$

The closure coefficients and source terms turbulence modeling are as given by [Yakhot *et al.* \(1992\)](#) for their κ - ε turbulence model based on Renormalization Group (RNG). Production rate of chemical species due to reactions is estimated using the law of mass action as

$$S_{Y_i} = W_i \left[(\gamma''_{ji} - \gamma'_{ji}) \left(k_{fj} \prod_{i=1}^N C_i^{\gamma'_{ji}} - k_{bj} \prod_{i=1}^N C_i^{\gamma''_{ji}} \right) \right]$$

An optimized eight-step H₂-O₂ finite chemistry reaction model proposed by [Evans and Schexnayder \(1982\)](#) is implemented in the present solver. Reaction rates of each reaction steps (k_f and k_b) are expressed in Arrhenius form. The thermodynamic properties are calculated the standard thermodynamic data of [McBride *et al.* \(1993\)](#). Total energy of the flow field is given by

$$E = \sum_{i=1}^{N_i} h_i Y_i - \frac{P}{\rho} + 0.5(u^2 + v^2)$$

Temperature is worked out from the above energy equation and the pressure in the flow field is calculated as

$$p = R_u \rho \sum_{i=1}^{N_i} \frac{Y_i T}{W_i}$$

4. NUMERICAL METHOD

The discretized form of governing equation based on Unstructured Finite Volume Method (UFVM) is

$$\int_{\Omega} \frac{\partial \mathbf{U}}{\partial t} d\Omega + \int_{\Gamma} |\mathbf{F}| \hat{n} d\Gamma - \int_{\Omega} \mathbf{S} d\Omega = 0 \quad (2)$$

where Γ and Ω are the surface area and volume of the cell respectively. The developed solver ([Deepu *et al.* 2006](#), [Shyji *et al.* 2017](#)) has now updated [[Deepu *et al.* \(2017\)](#)] with a low dissipative scheme for all speeds belongs to the family of Advection

Table 1 Nozzle inlet conditions

Flow parameter	Parameters of the propellants Injection to the thrust chamber		Inlet conditions to the nozzle	Species mass fractions at the nozzle inlet
	Fuel (H ₂)	Oxidizer (O ₂)		
Pressure (bar)	30.61	28.09	24.84	H ₂ =0.10499
Temperature (K)	285.6	502.5	3040.71	O ₂ =0.00031
Mass flow rate (kg/s)	0.1088	0.4178	0.5226	H ₂ O=0.87603
				OH=0.01558
				H=0.00267
				O=0.00042

Upstream Splitting Method (AUSM) developed by Liou and Steffen (1993), later modified as AUSM+up scheme (Liou 2006), is employed here to evaluate the inviscid fluxes by splitting them as a convective and pressure terms as

$$F = F^{(c)} + P \quad (3)$$

The pressure flux terms contain the interface pressure. Convective flux is represented in terms of convective Mach number M and the passive scalar quantities. This is represented using an interface mass flow rate $m_{1/2}$ and the convected vector quantity as

$$F^{(c)} = M \begin{bmatrix} \rho \\ \rho u \\ \rho v \\ \rho E \\ \rho k \\ \rho \varepsilon \\ \rho Y_i \end{bmatrix} = m_{1/2} \begin{bmatrix} 1 \\ u \\ v \\ E \\ k \\ \varepsilon \\ Y_i \end{bmatrix}$$

Explicit algorithms [Nair *et al.* (2010)] become inefficient while treating two phenomena (flow and reaction) of differing time scale together. In order to overcome this stiffness, a rescaling method proposed by Bussing and Murman (1988) is introduced here. Modified conservation equations upon integration takes the form

$$J \int_{\Omega} \frac{\partial \mathbf{U}}{\partial t} d\Omega + \int_{\Gamma} \mathbf{F} \hat{n} d\Gamma - \int_{\Omega} \mathbf{S} d\Omega = 0 \quad (4)$$

where J is the preconditioning matrix for the Jacobian of chemical species source terms considered in the present problem.

5. VALIDATION STUDIES

5.1 Sonic Wall Jet to Supersonic Free Stream

A benchmark experiment data from the studies of Aso *et al.* (1991) is chosen for the validation of the present solver, as it conforms to the objectives of the present studies on thrust augmentation by secondary injection. A secondary under expanded gaseous jet is admitted through a slot into a primary

supersonic cross flow. Two-dimensional Cartesian version of the present numerical code is used to simulate this validation test case. Supersonic inflow boundary condition is given at the inlet (M=3.75, P_{0f}=1.2MPa, and T₀=299K) and a sonic nitrogen jet (P_{0j}=0.31P_{0f} and T₀=299K) is given as a constant velocity jet boundary condition through a slot of 1mm width placed 330 mm from the leading edge. Two dimensional computational domain (429 mm ×165mm) was initially discretized with 370×120 control volumes. Grid is refined near jet and wall to maintain y⁺<1.0 in laminar sublayer. Later grid was refined to 520×205 and arrived at convergence in wall pressure profile as given Fig. 1. Numerical scheme is observed to be stable while solving such a problem involving complex flow physics and sharp gradients, with a maximum CFL of 0.45. Though the solver could predict the upstream pressure communication due to injection and the pressure recovery on floor after the expansion of the jet, the pressure rise due to the recirculation zone in the separation shock-boundary layer interaction region is slightly over predicted.

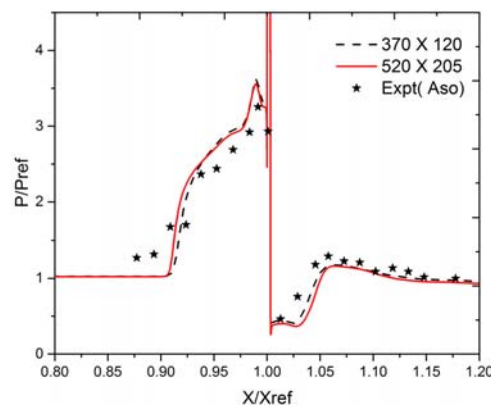


Fig. 1. Computed wall pressure distribution and its comparison with experiment.

5.2 Reacting Flow through a High Area Ratio H₂-O₂ Rocket Nozzle

Experimental data (Kacynski, 1994) reported for the wall pressure and hydrogen concentration for a 1030 area ratio Rao-contoured De-Laval Nozzle, developed by NASA LeRE, is used for the second level of validation of the solver. Nozzle contour for the computational is created from the data available

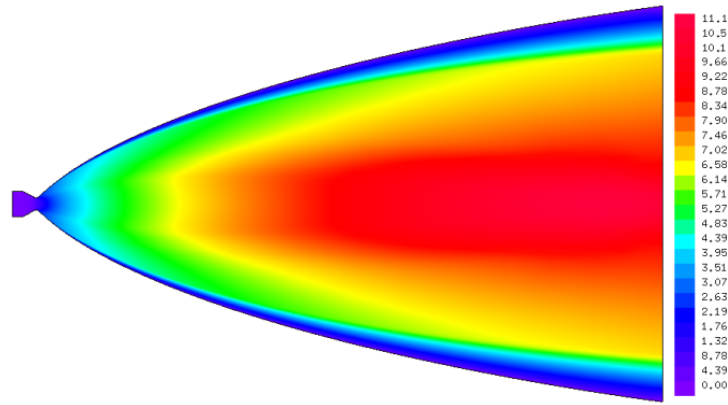


Fig. 2. Field plot for Mach number inside the nozzle.

from this experiment. Equilibrium composition corresponding to the thrust chamber operating conditions is worked out using Chemical Equilibrium Analysis (CEA) program developed by NASA. Boundary conditions specified at inlet of the computational domain is given in Table 1.

The computational domain was discretized in to 340×60 control volumes for the present validation test case. Entire flow domain was initialized with nozzle inlet conditions. Convergence for all conservation variables was observed after about 1,50,000 iterations while marching with CFL of 0.45. Number of iterations required was quite high due to uniqueness in flow development in high area ratio nozzle. Field plot of Mach number is given in Fig. 2. Dominance of viscous boundary layer is clearly observed here which limits the expansion of gas. Computed values of hydrogen concentration along nozzle wall (Fig. 3) agrees well with that reported in experiment (Kacynski, 1994). Higher pressure at the throat favor recombination of mono atomic hydrogen in combustion products, hence hydrogen concentration is observed to be high near the throat. Thereafter hydrogen concentration maintains the frozen value during the gas expansion in the diverging part of the nozzle.

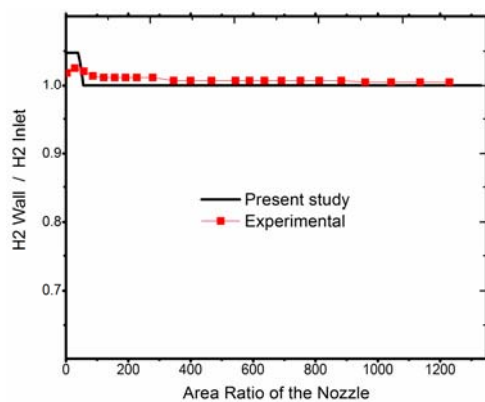


Fig. 3. Comparison of hydrogen concentration along nozzle wall with experiment (Kacynski, 1994).

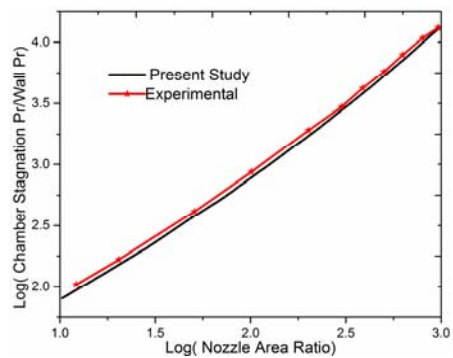


Fig. 4. Comparison of nozzle wall pressure distribution with experiment (Kacynski, 1994).

Computed nozzle wall pressure profile also agrees well with experimental measurements (Kacynski, 1994). The combustion chamber stagnation pressure to the wall pressure of the nozzle is plotted in logarithmic scale against the area ratio of the nozzle in the logarithmic scale. Nozzle wall pressure profile typical to perfectly expanded nozzle flow has been observed. Performance parameters of the nozzle obtained in the present study is compared and presented in Table 2. A close agreement of performance parameters is achieved in the present study as all possible loss mechanisms in nozzle such as divergence, turbulence, viscous effects, and species reaction are taken care of in the present study.

Table 2 Comparison of computed Performance parameters

Performance parameter	Present study	Experiment (NASA LeRE)	Analysis (Kacynski)
Mass flow rate, kg/s	0.5112	0.5226	0.5052
Vacuum thrust, N	2448	2422	2446.61
Specific impulse, s	479.0	469.9	493.6

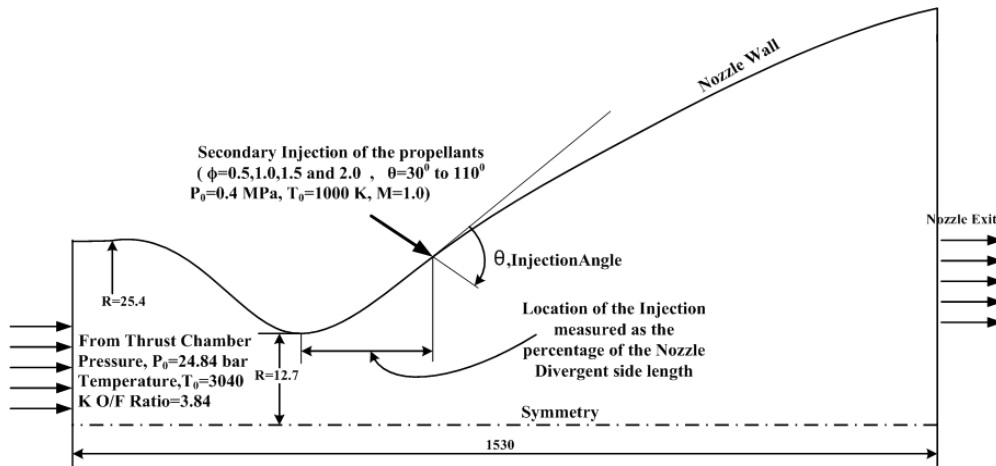


Fig. 5. Computational domain and boundary conditions used for thrust augmentation studies.

6. RESULTS AND DISCUSSION

6.1 Domain Discretization, Boundary Conditions, and Grid Independency Tests

Computational domain used for various simulation studies on thrust augmentation is given in Fig. 5. Nozzle inflow conditions are same as that used for validation study (Table 1). The species profile is worked out from Chemical Equilibrium Analysis corresponding to an oxidizer-fuel (OF) ratio of 3.84. Adiabatic, no-slip conditions are forced on nozzle wall. A sonic injection is given at a desired location from throat on nozzle wall as a constant velocity condition. Various jet conditions are used in the present study by varying angle of injection equivalence ratio of propellants, and pressure. A symmetry condition is given at bottom and conditions at supersonic exit are interpolated from the interior cells.

Computational domain was discretized with quadrilateral control volumes in four zones, in order to provide more grid density near throat, upstream and downstream of injection. Relatively coarser grid was used to discretize zone near to nozzle exit. Grid density is biased towards wall in all the zones so as to maintain $y^+ < 1$. A grid independency test has been performed for a sample test case with maximum injection angle (90°), as it exhibits maximum gradients in flow field. Computational domain was initially discretized to 170×30 control volumes and progressively refined to 260×45 , 340×60 and 420×75 control volumes. A comparison of thrust obtained for various level of discretization is given in Table 3. Since the variation in thrust in subsequent refinement beyond 340×60 control volumes was found to be minimal, it has been chosen for all thrust augmentation studies presented here.

6.2 Physics of sonic slot injection to expanding supersonic flow

Flow physics of sonic injection to supersonic free stream is quite well understood from various experimental and numerical studies. Whereas

secondary injection to expanding supersonic flow in nozzle for thrust augmentation exhibits diverse flow structures. This is due to the continuous expansion of free stream in diverging part of the nozzle and upstream communication of jet-boundary layer interaction. A schematic of flow field depicted based on present computational studies is given in Fig. 6.

Table 3 Grid independency tests

Grid	Number of divisions	Thrust estimated (N)
Coarse	170×30	2833
Medium	260×45	2854
Fine	340×60	2860
Very fine	420×75	2862

The secondary injection of the propellants obstructs the main flow through the nozzle and a bow shock is developed in the expanding flow. The interaction of this bow shock wave with the developing boundary layer creates a separation region near the secondary jet. Due to the boundary layer separation a separation shock wave is generated which causes shock-shock interaction phenomena. The boundary layer separation upstream of the jet has multiple vortices due to adverse pressure gradients in shock-boundary layer interaction and jet expansion. The secondary jet expands so as to match with local ambient pressure within the barrel shock and culminated by the Mach disc. Jet bends more in to the expanding main stream as it loses its momentum due to the formation of Mach disk. The depth of the Mach disk above the injection point can be considered as the extent of the jet penetration to the expanding main stream, which depends on pressure of the jet. Nozzle wall downstream vortices are generated due to the jet expansion which creates very low pressure on nozzle wall compared to that resulted by expanding nozzle flow. These pressure difference and vortices dies out further downstream of the jet.

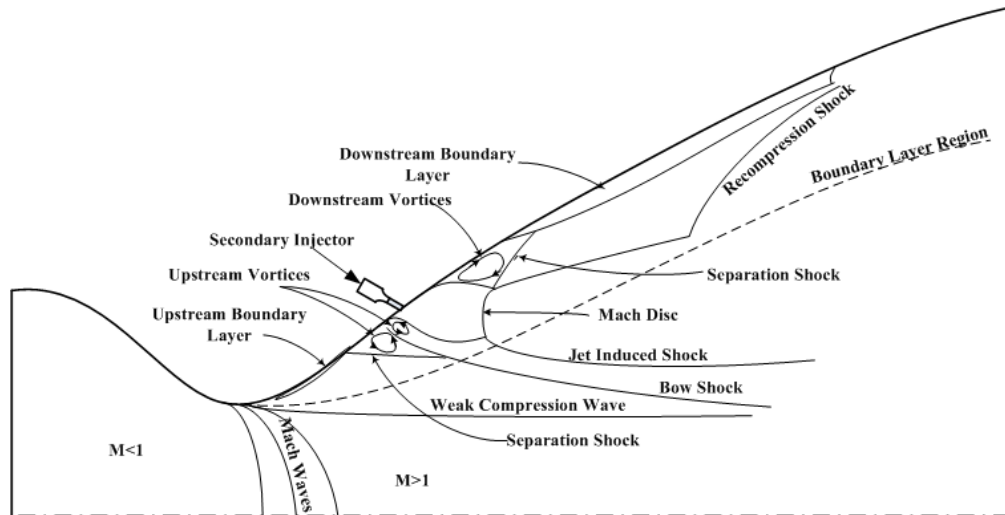


Fig. 6. Schematic of flow structures in sonic slot injection to expanding supersonic flow.

A comparison of wall pressure profile with injection and perfectly expanded nozzle flow is given in Fig. 7. This separated region in boundary layer is demarked by an associated separation shock generated from the upper tip of the Mach disk. The separation shock interacts with the nozzle wall where the boundary layer reattaches. This reattachment also generates a re-compression shock wave. The boundary layer gets thickened further as it develops towards the nozzle exit.

Field view of Mach number in a region close to injection point is given in Fig. 8. It can be seen that the aforementioned shock system and their interaction confines within the region close to the wall due to dominance of the momentum associated with expanding main flow. Therefore, the momentum losses due to injection are comparable to that happens in the boundary layer in a high area ratio nozzle.

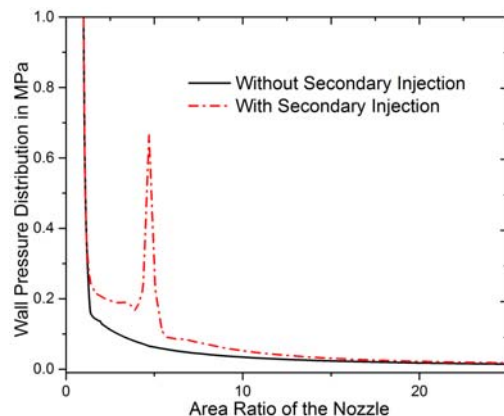


Fig. 7. Comparison of nozzle wall pressure distribution with and without injection.

Active combustion zones resulted by the secondary injection of propellants are examined in detail. Hydroxyl radical (OH) is already available at the

inlet of the nozzle due to the assumed equilibrium composition resulting by propellants burning in thrust chamber. Higher concentrations of OH radical exist in the region of high residence time and heat release (Fig. 9). Low velocity regions are indeed essential to promote reaction. Since the boundary layer regions have relatively low velocity in the entire region of flow inside high area nozzle, reaction activity gets confined near wall. Chemical reactions are observed to be nearly frozen in remaining areas of continuous expansion.

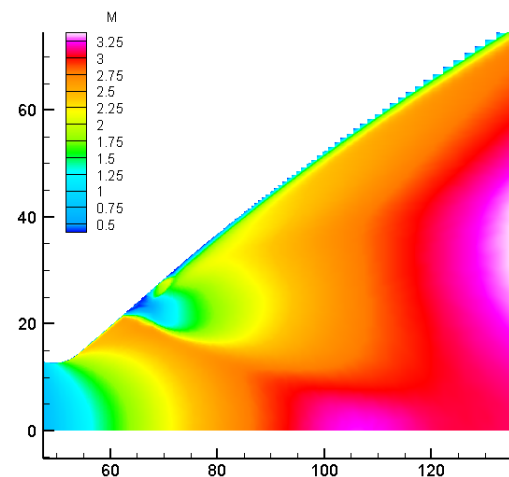


Fig. 8. Field plot for Mach number near injection point.

Field plot of temperature (Fig. 10) obviously shows burning of the secondary injected propellants even in the farther downstream locations from the injection point, which in turn augments the performance of the system. Expanding main flow acquires higher momentum and displaces burning regions close to the wall. This essentially calls for the requirement of special cooling systems for rocket nozzles with secondary injection.

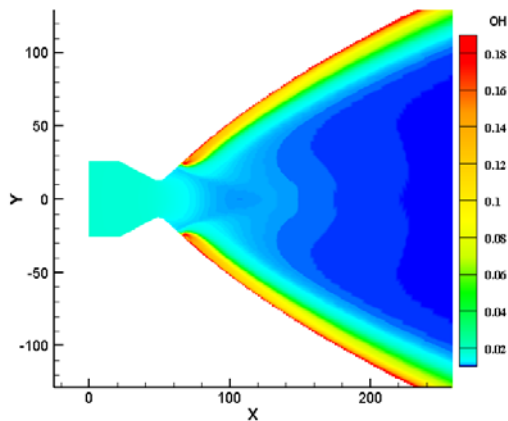


Fig. 9. Field plot for OH species in supersonic combustion in nozzle.

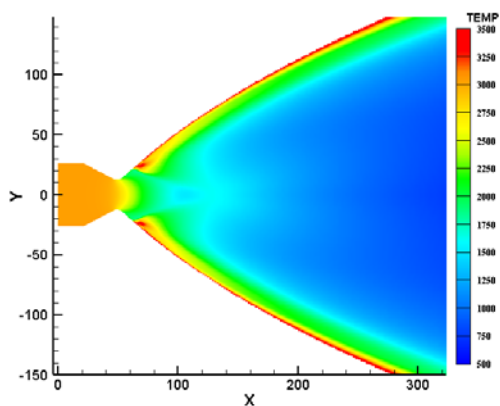


Fig. 10. Field plot for temperature for supersonic combustion in nozzle.

6.3 Performance Enhancement Due to Secondary Injection

Previous studies on thrust augmented rocket nozzle has established that the added mass, inertia and energy release associated with the combustion of the secondary injection of the propellants contributes to the exit thrust. Though the propellants in secondary injection can burn and contribute to delivered thrust, combustion of the propellants in the secondary injection flows parallel and close to the nozzle wall and displaces the core flow more towards the nozzle center. This in turn reduce the effective expansion ratio of the core flow compared to the actual geometry of the nozzle. Though the reduction in the effective expansion ratio of the nozzle brings substantial reduction in the average Mach number of the core flow, it increases the average nozzle exit pressure and compensates for the thrust losses due to the over expansion of the core flow. Displacement of core favor reduction in divergence loss. Gradients developed due to the introduction of secondary jet affects the momentum of nozzle flow. Therefore, there is always a tradeoff among the injection parameters in deciding the delivered performance due to the complex dynamics of the resulting flow field. Objective of the present study is to analyze various factors that influences augmentation of

thrust. Extensive numerical computations have been performed for various secondary injection parameters such as injection angle, pressure, equivalence ratio and position of injection.

6.4 Effect of Injection Angle in Thrust Augmentation

Pressure distribution on nozzle wall corresponding to various injection angles near to the injection point is given in Fig. 11. Structure of upstream vortices are observed to be different when the angle of injection is varied. Interaction point of separation shock is observed to shifting towards upstream when injection angle is increased and it results in an increase in size of upstream vortices. This happens due to the upstream communication of jet blockage in main nozzle flow and associated shift of bow and separation shocks. Downstream pressure recovery pattern is found to be identical for all injection angles as it depends primarily on extend of expansion of the jet.

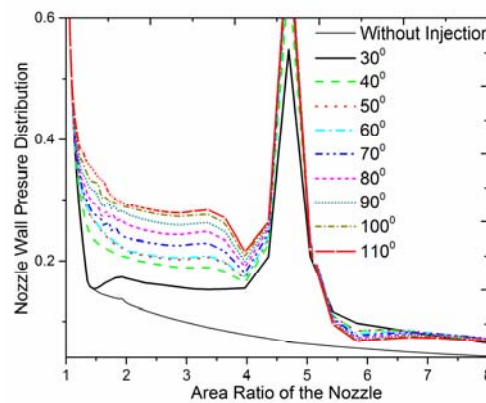


Fig. 11 Wall pressure distribution for various angle of injection.

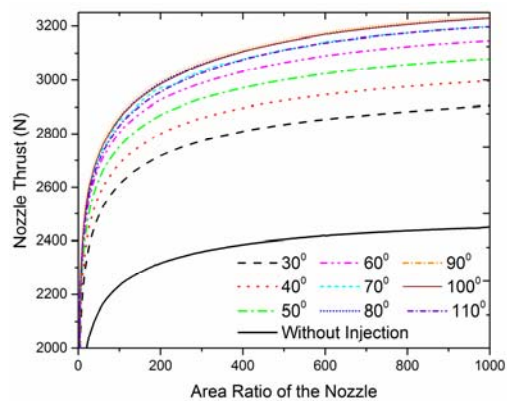


Fig. 12. Variation of nozzle thrust at various axial locations for different injection angle.

Thrust augmentation corresponding to various injection angles for a jet stream equivalence ratio of 1.5 is given in Fig. 12. Injection at higher angles enables mixing of injected stream, which is rich in fuel. Therefore, supersonic combustion downstream of the jet becomes more effective and produces more thrust. This trend is observed up to the

injections normal to the wall and subsequent injections at higher angles resulted in lower thrust. This is due to the momentum loss due to excessive blockage of main stream.

6.5 Effect of jet Stream Equivalence Ratio in Thrust Augmentation

Effect of jet stream equivalence ratio is studied for various injection angle. Fuel rich injection enables supersonic combustion with available oxygen in main nozzle flow. Maximum thrust production is achieved for an equivalence ratio of 1.5. Further increase in equivalence ratio resulted in poor performance due to incomplete combustion of propellant in secondary injection with main nozzle flow (Fig. 13). Peak performance is observed for normal injection for all equivalence ratios used in the simulations.

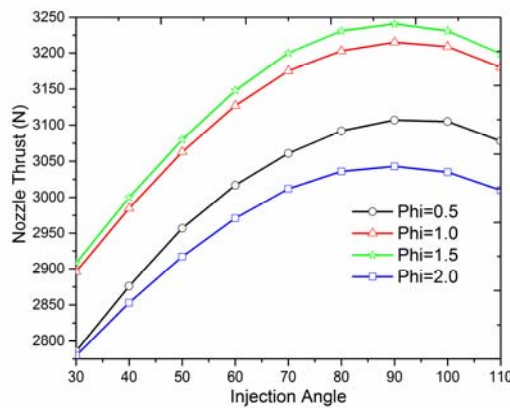


Fig. 13. Variation of nozzle thrust at exit for different injection angle and equivalence ratio.

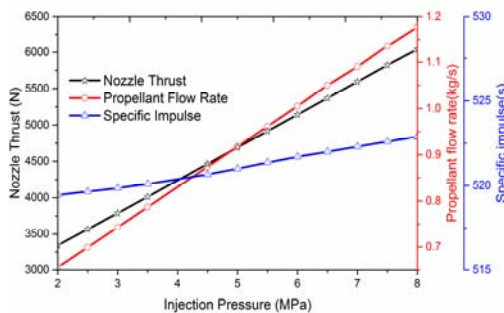


Fig. 14. Variation of delivered specific impulse for different injection pressure.

6.6 Effect of Secondary Jet Pressure in Thrust Augmentation

Numerical study was also extended to analyze the effect on injection pressure of secondary stream in nozzle performance. Performance augmentation is presented in Fig. 14. Though the nozzle thrust increases linearly with injection pressure, only a marginal rise is observed in specific impulse. This is due to the introduction of additional mass in secondary flow due to increase injection pressure. Marginal improvement in specific impulse at higher

injection pressure is attributed by the penetration and mixing of secondary jet in expanding main stream. This option is highly useful in nozzle thrust augmentation during the lift-off.

7. CONCLUSION

Numerical simulation of secondary injection to expanding supersonic flow in a high area ratio nozzle have been performed based on an indigenously developed solver. Following are the conclusion from thrust augmentation studies.

- Flow physics of sonic injection to expanding supersonic flow inside the diverging part of a high area ratio nozzle is simulated and salient flow structures are captured.
- AUSM+ -up scheme used in the present solver is robust in negotiating high gradients in the present simulation for under expanded jet interacting with expanding supersonic flow, even at higher time steps.
- Normal injection provides maximum performance due to enhanced mixing of secondary jet in main stream nozzle flow.
- Equivalence ratio of secondary jet can be fine-tuned based on unused oxidizer available in rocket thrust chamber for optimizing the thrust augmentation. Maximum thrust production is observed for an equivalence ratio of 1.5 in the present study.
- Nozzle thrust shows a consistent increase with ramping up of the injection pressure of the secondary jet. This option of pressure intensification does not have much effect on specific impulse due to the introduction of the additional mass flow.

REFERENCES

- Aso, S., S. Okuyama, M. Kawai and Y. Ando (1991) Experimental study on mixing phenomena in supersonic flows with slot injection, *AIAA 91-0016*.
- Aso, S., M. Tannou, S. Maekawa, Y. Ando, Y. Yamane and M. Fukuda (1994) A study on mixing phenomena in three-dimensional supersonic flow with circular injection, *AIAA-94-0707*.
- Boles, J. A., J. R. Edwards and R. A. Bauerle (2010). Large-eddy/Reynolds-averaged Navier-Stokes simulations of sonic injection into Mach 2 crossflow. *AIAA journal*, 48(7), 1444-1456.
- Borowski, S. K., R. R. Corban, D. W. Culver, M. J. Bulman and M. C. Mcilwain (1994). A revolutionary lunar space transportation system architecture using extraterrestrial LOX-augmented NTR propulsion, *AIAA-94-3343, 30th AIAA/ASME/SAE/ASEE Joint Propulsion Conference*.

- Bulman, M. J., T. M. Neill and S. K. Borowski (2000). Simulated LOX-augmented nuclear thermal rocket (LANTR) testing. *AIAA 2000-3897, 36th AIAA/ASME/SAE/ASEE Joint Propulsion Conference 16-19*.
- Bussing, T. R. A. and E. M. Murman (1988). Finite Volume Method for the Calculation of Compressible Chemically Reacting Flows, *AIAA Journal* 26, 1070-1078.
- Candon, M. J. and H. Ogawa (2015). Thrust augmentation optimization through supersonic after-burning in scramjet engine nozzles via surrogate-assisted evolutionary algorithms. *Acta Astronautica* 116, 132-147.
- Davis, R. L., M. J. Bulman and C. Yam (2006). Numerical simulation of a thrust augmented rocket nozzle. *AIAA* 5205.
- Deepu, M. N., S. S. Gokhale and S. Jayaraj (2007). Numerical modelling of scramjet combustor, *Defence Science Journal* 57(4), 367-379.
- Deepu, M., M. P. Dhrishit and S. Shyji (2017). Numerical simulation of high speed reacting shear layers using AUSM+ scheme-based unstructured finite volume method solver, *International Journal of Modeling, Simulation, and Scientific Computing* 8(4), 1750020.
- Evans, J. S. and C. J. Schexnayder (1980). Influence of Chemical Kinetics and Unmixedness on Burning Supersonic Hydrogen Flames, *AIAA Journal* 18(2), 188-193.
- Everett, D. E., M. A. Woodmansee, J. C. Dutton and M. J. Morris (1998). Wall pressure measurements for a sonic jet injected transversely into a supersonic crossflow. *Journal of Propulsion and Power* 14(6), 861-868.
- Forde, S., M. Bulman and T. Neill (2006). Thrust augmentation nozzle (TAN) concept for rocket engine booster applications. *Acta Astronautica*, 59(1), 271-277.
- Fuller, R. P., P. K. Wu, K. A. Kirkendall and A. S. Nejad (2000). Effects of injection angle on atomization of liquid jets in transverse airflow. *AIAA journal* 38(1), 64-72.
- Gao, Z. and C. Lee (2011). Numerical research on mixing characteristics of different injection schemes for supersonic transverse jet. *Science China Technological Sciences* 54(4), 883-893.
- Gruber, M. R., A. S. Nejad, T. H. Chen and J. C. Dutton (1995). Mixing and penetration studies of sonic jets in a Mach 2 freestream. *Journal of Propulsion and Power* 11(2), 315-323.
- Kacynski, K. J. (1994). Calculation of Propulsive Nozzle Flow fields in Multi diffusing Chemically Reacting Environments, *Ph.D. Thesis, Purdue University*.
- Liou, M. S. (2006). A sequel to AUSM, Part II: AUSM+ up for all speeds. *Journal of Computational Physics* 214(1), 137-170.
- Liou, M. S. and C. J. Steffen (1993). A new flux splitting scheme. *Journal of Computational physics* 107(1), 23-39.
- McBride, B. J., S. Gordon and M. A. Reno (1993). Coefficients for calculating thermodynamic and transport properties of individual species.
- Nair, P., T. Jayachandran, M. Deepu, B. P. Puranik and U. V. Bhandarkar (2010). Numerical simulation of interaction of sonic jet with high speed flow over a blunt body using solution mapped higher order accurate AUSM+UP based flow solver. *Journal of Applied Fluid Mechanics* 3(1), 15-23.
- Pavli, A. J., K. J. Kacynski and T. A. Smith (1987). Experimental thrust performance of a high-area-ratio rocket nozzle, *NASA-TP-2720*.
- Rizetta, D. P. (1992). Numerical simulation of slot injection into a turbulent supersonic stream. *AIAA journal* 30(10), 2434-2439.
- Shyji, S., N. A. Kumar, T. Jayachandran and M. Deepu (2017). Reacting Flow Simulation of Rocket Nozzles. *Fluid Mechanics and Fluid Power—Contemporary Research* 1485-1495. Springer India.
- Spaid, F. W. and E. Zukoski (1964). Secondary injection of gases into a supersonic flow. *AIAA journal* 2(10), 1689-1696.
- Yakhot, V. S. A. S. T. B. C. G., S. A. Orszag, S. Thangam, T. B. Gatski and C. G. Speziale (1992). Development of turbulence models for shear flows by a double expansion technique. *Physics of Fluids A: Fluid Dynamics (1989-1993)*, 4(7), 1510-1520.